

Configurations of adsorbed hard spheres after diffusion in a gravitational field

(random walk/coverage/distribution function/Monte Carlo)

B. SENGER[†], F. J. BAFALUY^{†‡}, P. SCHAAF^{§¶||}, A. SCHMITT[§], AND J.-C. VOEGEL[†]

[†]Institut National de la Santé et de la Recherche Médicale, Unité no. 157, Faculté de Chirurgie Dentaire, 1, place de l'Hôpital, 67000 Strasbourg, France; [‡]Departament de Física, Universitat Autònoma de Barcelona, 08193 Bellaterra, Spain; [§]Institut Charles Sadron, 6, rue Boussingault, 67083 Strasbourg Cédex, France; and [¶]Ecole Européenne des Hautes Etudes des Industries Chimiques de Strasbourg, 1, rue Blaise Pascal, BP 296F, 67008 Strasbourg Cédex, France

Communicated by B. Widom, May 18, 1992 (received for review March 25, 1992)

ABSTRACT The deposition and adhesion of particles on a solid surface are governed by a great number of interplaying forces. In this paper we analyze, by means of computer simulations, the influence of (i) the short-range repulsive forces, modeled by hard sphere interactions, (ii) the gravitational forces, and (iii) the diffusion process of the particles in the fluid on the structure of the surface covered by the particles. In particular, the evolution of the limiting coverage, Θ_∞ (where Θ is the reduced relative surface coverage), and the radial distribution, $g(r)$, at the jamming limit, are determined as a function of the gravitational forces. These forces play an important role in many experiments performed on latex beads. Our results should stimulate new experiments in this field and, thus, be directly experimentally tested. It is shown, for example, that for polystyrene particles Θ_∞ is constant and equal to the random sequential adsorption jamming limit value for radii R not larger than $1 \mu\text{m}$. It increases for $1 \leq R \leq 3 \mu\text{m}$ and tends, for higher R , to a plateau, whose value is approximately equal to 0.61. The tendency to a closer packing when R is large, and thus large gravitational forces, is confirmed by the shape of the radial distribution function. This phenomenon occurs not only for jammed surfaces but also for unsaturated surfaces.

1. INTRODUCTION

Adsorption of particles (latex beads, bacteria, globular proteins, etc.) has a wide variety of applications in materials sciences as well as in biology or biotechnology. Since the pioneering works of Rényi (1) and Palastý (2), many efforts have been devoted to the theoretical and numerical modeling of the adhesion of particles of colloidal size on planar surfaces. In this article, we are interested in the numerical study of the adhesion of spherical particles such as latex beads on planar surfaces, in the absence of an external flux. Due to the great variety of the forces playing a role in these processes, their study is still in a native stage. These processes are mainly governed by (i) random fluctuating forces leading to the Brownian motion of the particles in the fluid, (ii) interparticle forces, including hydrodynamic forces, van der Waals forces, Coulombic interactions, (iii) gravitational forces, and (iv) finally, the interactions between the particles and the adhesive surface.

Following Rényi and Palastý, the principal models that were developed up to now are directly related to the random sequential adsorption (RSA) algorithm. It has been suggested by Feder and Giaever (3) to describe the adsorption of proteins on solid surfaces and by Onoda and Liniger (4) to model the adhesion of latex beads on planar surfaces. The RSA model takes into account the fact that two particles

cannot overlap. Thus, it includes the short-range repulsive forces. None of the other forces mentioned above, however, is incorporated in this model. A first approach to include van der Waals and Coulombic interactions has been developed by Adamczyk *et al.* (5), who studied the adsorption of charged disks. More recently, we proposed a model [diffusion RSA (DRSA)] of sequential adsorption including the diffusion of the particles (spheres) in the bulk (on a three-dimensional fine mesh grid) prior to their adsorption on a flat surface (6, 7). These studies showed that the diffusion does not modify either the coverage at jamming, Θ_∞ (Θ being the reduced relative surface coverage), or the corresponding distribution of radial distances, $g(r)$, with respect to their RSA counterparts. In contrast, at coverage smaller than Θ_∞ , the $g(r)$ functions based on DRSA and RSA differ significantly. This has been investigated theoretically by Tarjus and Viot (8) in a two-dimensional space, the adsorption surface being a line.

One of the current problems in this field is to relate predictions to experimental results. The method best adapted to this purpose is the optical microscopy. But this usually implies that the particles have a diameter of the order of, or larger than, $1 \mu\text{m}$. For latex beads, however, which are commonly available, the gravity has then an effect on the deposition process. Thus, it is the joint effect of gravity, Brownian motion of the particles in the fluid, and short-range repulsive forces on the adhesion process that will be analyzed in this paper. This work appears as an important extension of our previous DRSA model. We neglect, however, the contribution from hydrodynamic forces, van der Waals, and Coulombic interactions between particles. We assume, as suggested by our observations (P.S., unpublished data), that once the particles touch the adhesion surface, they are irreversibly fixed on it. We will only be interested in structural aspects of the surface covered by the particles. The kinetic aspects are more difficult to analyze because the interactions between the particles in the stage of adsorption and the particles from the solution have to be taken into account, unless the solution is very dilute, which is a situation of minor experimental interest.

In Section 2, we describe additional aspects of the model that has been used. The simulations were performed on a lattice. The dependence on the gravity of the transition probabilities in one of the six possible directions will, in particular, be discussed. A similar approach has been used by Huang and Somasundaran (9), who restricted the displacement to the four orthogonal directions available in a vertical plane, to study the sedimentation process by means of a discrete model, where gravitation and Brownian motion were considered. The results we obtained by means of the proposed simulation model are presented in Section 3. Emphasis

The publication costs of this article were defrayed in part by page charge payment. This article must therefore be hereby marked "advertisement" in accordance with 18 U.S.C. §1734 solely to indicate this fact.

Abbreviations: RSA, random sequential adsorption; DRSA, diffusion RSA.

||To whom reprint requests should be addressed.

is placed on the coverage at jamming (Section 3.1). It is, in particular, shown that Θ_∞ stays constant up to a particle radius of $\approx 1 \mu\text{m}$ (in the case of polystyrene particles), before rising quite rapidly for larger values of R . It reaches a plateau whose relative coverage is of the order of 0.61, for radii larger than approximately $3 \mu\text{m}$. For such particles, the gravity is the dominant effect governing the deposition process. In Section 3.2, we compare the radial distribution functions, $g(r)$, at the jamming limit for different values of R , and thus different contributions from gravity. It reveals a first important peak in $g(r)$ that grows systematically with R and a second peak shifting slowly from an abscissa larger than $4R$ to $4R$, when R increases. Both observations confirm the closer packing obtained with large particles with respect to smaller ones. Some concluding remarks are proposed in Section 4.

2. SIMULATION MODEL

The geometry of the simulation model has already been described elsewhere (6, 7) and only will be recalled shortly here. In this previous study, however, no gravity was incorporated in the model. The particles (spheres of radius R) move on a three-dimensional grid with cubic meshes of side δ ; the center of the particles can only occupy the nodes of this grid. At each step the center moves to one of the six neighboring nodes unless this step leads to an overlap of the moving sphere with one of the already adsorbed particles, by virtue of the hard-core interaction between particles. Once the particle touches the surface, it remains fixed and keeps its position during the whole process, up to the obtention of a jammed surface. Each particle starts randomly at a height equal to $3R$. Indeed, the particles diffusing from the bulk to the surface, and reaching for the first time the plane $z = 3R$, have never touched before the already adsorbed particles. They are thus randomly distributed over it. This would not be the case if long-range forces would be taken into account. The particles are considered as lost if their centers reach an altitude of $5R$. This avoids undue prolonged computing time. Furthermore, periodic boundary conditions are applied to the vertical walls of the box, that are perpendicular to the adsorbing bottom surface, which is a square of dimensions $c \times c$. This length has been chosen throughout the computations presented here so as to verify the relation $c^2 \approx 100\pi R^2$.

In the case where a particle is subjected only to the random collisions with the fluid molecules (pure Brownian motion), the probabilities for jumping from its position to one of the six adjacent nodes are equal to $1/6$ *a priori* [so-called "blind walker" (10)]. Obviously, if the particle is submitted to its weight (or more generally to a deterministic external force in the Oz direction) in addition to the random force, the space is no longer isotropic, and the probabilities associated to this direction significantly differ from the four others. As a consequence, it is assumed that the probability P of making a step in a given direction (hereafter denoted by x^+ , x^- , y^+ , y^- , z^+ , or z^-) depends upon the corresponding variation of potential ΔU :

$$P \sim e^{-\Delta U/2kT} \quad [1]$$

and

$$\Delta U/kT = (4/3)\pi R^3 \Delta \rho g \delta z / kT, \quad [2]$$

k represents the Boltzmann constant, T the absolute temperature, $\Delta \rho$ the difference between the specific mass of the particles and that of the liquid medium containing the particles, g is the acceleration of gravity, and δz is the altitude variation corresponding to the step. If the step occurs in the horizontal plane (i.e., a plane parallel to xOy), $\Delta U = 0$. If the

displacement occurs along the vertical axis, δz is either $+\delta$ or $-\delta$, depending on whether the particle moves upward (z^+ direction) or downward (z^- direction). The factor 2 appearing in Eq. 1 is needed so that the master equation corresponding to this process leads to the well-known Smolukowski equation after the correspondence between $\delta^2/6\delta t$ and the diffusion coefficient D of the particles in the medium has been made. δt represents the characteristic time associated to one computer step. The jump probabilities associated to the different possible steps are then:

$$\begin{aligned} P(x^+) &= P(x^-) = P(y^+) = P(y^-) = 1/(4 + e^A + e^{-A}) \\ P(z^+) &= e^{-A}/(4 + e^A + e^{-A}) \\ P(z^-) &= e^A/(4 + e^A + e^{-A}), \end{aligned} \quad [3]$$

where $A = (4/3)\pi R^3 \Delta \rho g \delta z / 2kT$ has been introduced to simplify the notation. With the various definitions given above, the detailed balance condition $P(z^+)/P(z^-) = e^{-2A} = e^{-\Delta U/kT}$ is satisfied and, as a consequence, the equilibrium probability distribution is the Boltzmann distribution. Note that for $A = 0$, all probabilities equal $1/6$ (pure Brownian movement without gravitational force), and for $A \rightarrow \infty$, $p(z^-) \rightarrow 1$ (deterministic vertical fall).

To avoid undesirable effects due to the discretization of the space, the step length δ must be small if compared to the sphere radius R . We therefore set $\delta = \epsilon R$, where ϵ is a dimensionless parameter small with respect to 1. The parameter A varies then as $R^4 \Delta \rho \epsilon$. In the following, $\Delta \rho$ is fixed to 45 kg/m^3 (i.e., 0.045 g/cm^3) corresponding to polystyrene beads in water and T is fixed to 300 K. Thus only two parameters are free (R and ϵ), and all results will be discussed with respect to their values.

The probabilities defined above are used in the Monte Carlo computer code written for simulating the random walk of particles in a fluid and their adsorption on a flat surface. The position of each adsorbed particle is stored during the simulation and is available for the determination of various characteristics of the process, as described in the following section.

Prior to the simulations aimed at gradually covering the surfaces, we have simulated the trajectories of particles above empty surfaces and recorded the number of steps they needed for adsorbing on them. These numbers were compared to those determined theoretically for various values of A , which takes all of the parameters into account, as shown in Appendix.

3. RESULTS

In this section, we present results related to the configurations of the particles adsorbed after diffusion in the bulk. Thus, two quantities are of special interest: the coverage at the jamming limit, Θ_∞ (Section 3.1) and the radial distribution function, $g(r)$ (Section 3.2). Owing to the strong variance inherent to the process described, large samples of surfaces have to be produced to reduce the uncertainty on coverage and radial distribution function and thus to allow significant comparisons.

3.1. Coverage at the Jamming Limit. In principle, particle trajectories are simulated as long as the surfaces are not entirely covered. However, as is well known, the time needed to adsorb a particle increases dramatically at the end of the process. To avoid prohibitive computer times, the simulations were stopped when only small targets [areas of the order of a few $(\epsilon R)^2$] were still free on the surface for the center of a new particle. These targets were filled by using a RSA algorithm—i.e., by randomly placing a sphere in them without any diffusion process of the particle in the neighborhood of the surface. This procedure (described in detail in

refs. 6 and 7) does not alter the statistical significance of the particle configuration obtained but only the dynamics of the process (not considered here). For each combination (R , ϵ) examined, 200 surfaces were covered, leading, on the average, to a 95% confidence interval whose half-width represents $<0.5\%$ of Θ_∞ .

To provide an easy way to predict the jamming limit coverage for any combination of the parameters, the physical radius R has been replaced by a dimensionless radius R^* defined by:

$$R^* = R(4\pi\Delta\rho g/3kT)^{1/4}, \quad [4]$$

where the scaling factor amounts to $\approx 0.817411 \mu\text{m}^{-1}$ for our conditions. Therefore, R (in μm) and R^* are expressed by figures of the same order of magnitude.

Fig. 1 shows the values of Θ_∞ obtained for R^* ranging from 0 up to ≈ 5 and ϵ values equal to 1/10, 1/25, 1/50, 1/100, and 1/200. Three main regions can be recognized on the graph:

(i) For $R^* \leq 1$, the coverage stays nearly constant, equal to the usual value of $\Theta_\infty \approx 0.546$ obtained with models in a continuous space (11); it seems therefore not to be affected by the discretization introduced in the present work, at least not with the ϵ values taken into account. In this region, the weight of the particle does not disturb the Brownian motion.

(ii) For $1 \leq R^* \leq 3$, the coverage rises with R^* , since the gravitational force plays an increasing part and dominates progressively the random displacement of the particles.

(iii) Finally, for $R^* \geq 3$, Θ_∞ reaches a plateau whose height is $(\Theta_\infty)_{\text{max}} = 0.6099 \pm 0.0023$, which is compatible with the estimation of Jullien and Meakin (12) who found 0.61056 ± 0.00005 .

It appears that the coverage at jamming is independent of ϵ , showing thus that the mesh size is sufficiently small to render the discrete model a satisfactory approximation of a continuous one.

By means of the same model it is also possible to study the coverage against a negative gravitational effect, by choosing a specific mass of the particles smaller than that of the fluid. In this case, the probability to adsorb decreases rapidly and most particles escape toward the top surface of the fluid. We could nevertheless show that for low values of A (-0.005 and -0.01) and for $\epsilon = 1/25$, the coverage at jamming was 0.546 within the statistical fluctuations—i.e., the same value as in the absence of gravity. The combinations (A , ϵ) indicated above, for $\Delta\rho = -0.045 \text{ g/cm}^3$, correspond to $R \approx 0.865 \mu\text{m}$ ($R^* \approx 0.707$) and $R \approx 1.029 \mu\text{m}$ ($R^* \approx 0.841$), respectively.

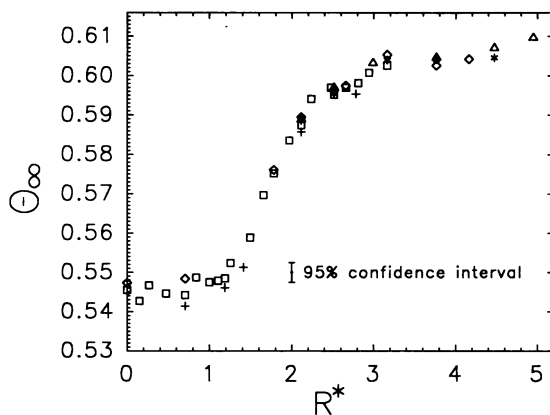


FIG. 1. Variation of the coverage Θ_∞ at the jamming limit as a function of the particle radius R , expressed as a dimensionless radius R^* (see Eq. 4), for different values of the step length δ expressed as the fraction ϵ of R ($\epsilon = \delta/R$): +, $\epsilon = 1/10$; □, $\epsilon = 1/25$; ◇, $\epsilon = 1/50$; *, $\epsilon = 1/100$; △, $\epsilon = 1/200$.

3.2. Radial Distribution Function. The radial distribution function, $g(r)$, is a convenient means for representing the relative position of particles deposited onto a surface. It reflects the eventual correlation existing between the particles—i.e., the tendency to group [peaks of $g(r)$]—as well as the disappearance of the correlation at large separations [$g(r) \approx 1$]. The definition adopted is the classical one, as proposed for instance in ref. 11. It must, however, be emphasized that, $g(r)$ being built up on the basis of the distance frequency distribution, which is a histogram, it is itself given in a histogrammatic form; the height in a given distance class is the average (not the sum) over this class. Since the frequencies derived from the simulations are necessarily finite, $g(r)$ becomes not infinite at contact (i.e., when $r \rightarrow 2R^+$) but displays anyhow a steep slope. In the following, we present $g(r)$ derived from our simulations, in the case of jammed surfaces (Section 3.2.1) as well as at lower relative coverage (Section 3.2.2).

3.2.1. Distributions for jammed surfaces. The radial distribution functions, $g(r)$, have been determined for 200 surfaces covered up to saturation, for various values of R and ϵ . Fig. 2 shows $g(r)$ for $R \approx 0.865$, 2.587, and 6.055 μm ($R^* \approx 0.707$, 2.115, and 4.949, respectively), corresponding to the three typical regions of Θ_∞ as a function of R (see Fig. 1). It appears clearly that $g(r)$ is practically insensitive to ϵ . Therefore, curves corresponding to only two values of ϵ are represented in Fig. 2. It must be noted that in each case, the $g(r)$ values are mean values obtained in an annulus of inner radius r and of width $\Delta r = R/5$. It can be seen that the first peak increases with R , thus revealing the tendency of the large particles to pack closer than the smaller ones. The explanation of this behavior is very simple. Indeed, a diffusing particle that hits an adsorbed particle will land closer to that particle if the effect of gravity is strong. In the limit of infinitely strong gravity, it will be adsorbed in contact with the particle that it hit. This effect is also responsible for the higher jamming limit coverage observed with strong gravity mentioned above. It is also quite clear that when R decreases, $g(r)$ tends to a flat distribution corresponding to point particles for which, obviously, the gravitational effect vanishes. Another observation, which confirms the relative strong packing of the large particles, is that the second peak (Fig. 2) which occurs at $r \approx 4.4R$ when $R = 0.865 \mu\text{m}$, shifts toward $r = 4R$ when R increases and sharpens accordingly.

3.2.2. Distributions for nonjammed surfaces. We have also examined surfaces that were not completely covered. In this case, a larger number of surfaces had to be generated to compensate for the lower number of particles available. Thus 1200 surfaces with 25 particles per surface were produced for $R \approx 0.865$, 2.587, and 6.055 μm . The $g(r)$ functions corresponding to these radii, and to a coverage of ≈ 0.2424 , are represented in Fig. 3. The same computations were carried out on 35,000 surfaces covered to ≈ 0.04848 . In both cases, the $g(r)$ functions behave qualitatively in a similar manner as for $\Theta = \Theta_\infty$.

4. CONCLUSION

This work is related to the widely explored problem of the adhesion of particles of various shapes onto surfaces, generally under the sole action of the Brownian (i.e., random) forces exerted by the fluid molecules on the particles in suspension. This phenomenon occurs for mineral or organic particles as well as for biological objects such as proteins, bacteria, and cells.

We studied the adsorption of hard spherical particles onto a flat surface, under the combined influence of the Brownian collisions with the fluid molecules and of the gravitational force, for fixed temperature and difference of specific gravity

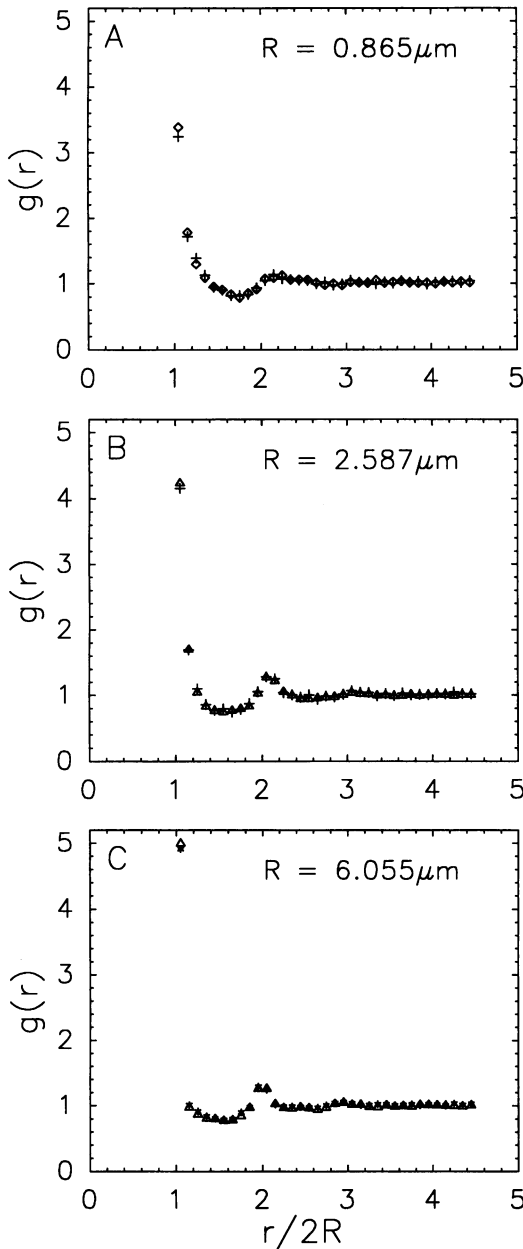


FIG. 2. Radial distribution function $g(r)$, for 200 jammed surfaces as a function of the reduced sphere center-to-center distance $r/2R$, for various values of the sphere radius R and of the relative fine-mesh grid size ϵ (symbols as in Fig. 1).

between the particle material and the bulk. The diffusion of the particles and their adsorption were numerically simulated on a three-dimensional grid whose mesh was small with respect to the particle radius R . The latter ranged from 0 (absence of gravity) up to $\approx 6 \mu\text{m}$, where the gravity dominates the probability of jumping from one node to a neighboring one. By means of these computer simulations, it was shown that the coverage at saturation, Θ_∞ , stayed nearly equal to the well-known value of ≈ 0.546 for small particles ($R^* \leq 1$) and increased quite rapidly up to ≈ 0.61 for larger particles.

The increase of packing at saturation, revealed by the behavior of the coverage, is entirely reflected by the radial distribution function, $g(r)$, that displays peaks that emerge more and more significantly when R increases. It is worth noting that this property was also verified for surfaces covered to only $\approx 24\%$ and even $\approx 4.8\%$. Finally, it may be mentioned that for a small negative gravitational force (i.e.,

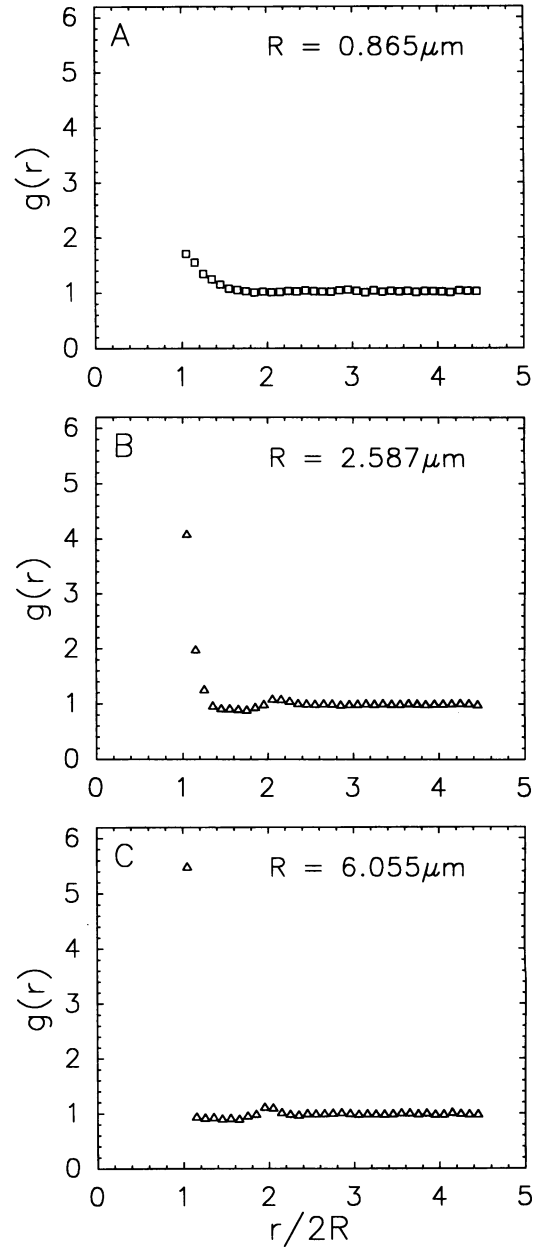


FIG. 3. Radial distribution function $g(r)$, for 1200 surfaces covered to $\approx 24\%$ as a function of the reduced sphere center-to-center distance $r/2R$, for various values of the sphere radius R and of the relative fine-mesh grid size ϵ (symbols as in Fig. 1).

directed upward), the simulations predicted a coverage that stayed constant, equal to 0.546 within the statistical fluctuations.

APPENDIX

We have determined the mean number of steps that a particle makes going from its starting point ($z = 3R$) to its end point ($z = R$) when the adsorption occurs on an empty surface. Consider an interval of length $L = 4R$ and a particle initially located in its middle ($z = 2R$); the interval is subdivided in steps of length ϵR . Conversely, one can also take one step as length unit and then ascribe to the particle the dimensionless radius $R/\epsilon R = 1/\epsilon$; the length of the interval is then $4/\epsilon$ and the starting point is $z = 2/\epsilon$. Adapting a formula given by Feller (13) to this case leads to the mean number of steps $\langle n_{1D} \rangle$ needed for the particle to reach one of the barriers “ $z = 0$ ”

or " $z = 4/\varepsilon$ ". In this one-dimensional problem, the probabilities p and q to make a step in the positive or negative direction of the z axis are given by:

$$\begin{aligned} p &= e^{-A}/(e^A + e^{-A}) \\ q &= e^A/(e^A + e^{-A}). \end{aligned} \quad [\text{A1}]$$

While keeping the proportionality to e^{-A} or e^A as in section 2, the normalization to 1 modifies the expression of the probabilities if compared to the three-dimensional case. One obtains then:

$$\langle n_{1D} \rangle = 2 \tanh(2A/\varepsilon)/[\varepsilon \tanh(A)]. \quad [\text{A2}]$$

In the absence of gravity ($A = 0$), a Taylor expansion of this equation leads to:

$$\langle n_{1D}(A = 0) \rangle = 4/\varepsilon^2. \quad [\text{A3}]$$

The three-dimensional space is then isotropic and the mean number of steps $\langle n_{3D} \rangle$ of a particle that reaches the barrier (i.e., the adsorbing surface) is merely:

$$\langle n_{3D}(A = 0) \rangle = 3 \langle n_{1D}(A = 0) \rangle = 12/\varepsilon^2. \quad [\text{A4}]$$

When the gravitational force acts on the particle the passage from $\langle n_{1D} \rangle$ to $\langle n_{3D} \rangle$ is obtained by:

$$\langle n_{3D} \rangle = \langle n_{1D} \rangle [4P(x^+) + P(z^+) + P(z^-)] [P(z^+) + P(z^-)]^{-1}. \quad [\text{A5}]$$

Table 1. Comparison between the numbers of steps made by a particle for adsorbing on an empty surface, derived from simulations ($\langle n_{3D} \rangle_{\text{sim}}$) and theory ($\langle n_{3D} \rangle_{\text{th}}$), as a function of the parameters A and ε

A	$\varepsilon = 1/25$		$\varepsilon = 1/200$	
	$\langle n_{3D} \rangle_{\text{sim}}$	$\langle n_{3D} \rangle_{\text{th}}$	$\langle n_{3D} \rangle_{\text{sim}}$	$\langle n_{3D} \rangle_{\text{th}}$
0	7591.6	7500.0	499551.8	480000.0
0.001	7519.8	7493.8	468012.0	455938.8
0.01	7113.6	6931.8	120854.0	119919.5
0.1	1529.7	1499.9	12036.4	12000.0
1	151.3	150.7	1204.8	1205.9
5	51.4	51.4	411.0	410.8

Inserting the probabilities defined by Eq. 3, one obtains:

$$\langle n_{3D} \rangle = \langle n_{1D} \rangle (4 + e^A + e^{-A}) (e^A + e^{-A})^{-1}. \quad [\text{A6}]$$

Obviously, $\langle n_{3D}(A = \infty) \rangle = \langle n_{1D}(A = \infty) \rangle$, since the lateral displacements are completely excluded. Inserting Eq. A2 into Eq. A6 leads finally to:

$$\langle n_{3D} \rangle / \langle n_{3D}(A = 0) \rangle = \varepsilon \tanh(2A/\varepsilon) [2 + \cosh(A)] / [6 \sinh(A)]. \quad [\text{A7}]$$

Values of $\langle n_{3D} \rangle$ derived by means of Eqs. A4 and A7 are given in Table 1 for $\varepsilon = 1/25$ and $1/200$ and a series of values of A . They are compared to the corresponding numbers of steps obtained by simulations. It can be seen that both agree within a few percent.

We are indebted to Professor J. Talbot for helpful discussions. This work has been partly supported by North Atlantic Treaty Organization Grant 890872. Two of us (P.S. and F.J.B.) acknowledge the Commission of the European Communities for its financial support [Contract SC1-CT-91-0696(TSTS) and Contract SC1-915166, respectively].

1. Rényi, A. (1958) *Publ. Math. Inst. Hung. Acad. Sci.* **3**, 109–127.
2. Palasti, I. (1960) *Magy. Tud. Akad. Mat. Kut. Intéz. Közl.* **5**, 353–359.
3. Feder, J. & Giaever, I. (1980) *J. Colloid Interface Sci.* **78**, 144–154.
4. Onoda, G. Y. & Liniger, E. G. (1986) *Phys. Rev. A* **33**, 715–716.
5. Adamczyk, Z., Zembala, M., Siwek, B. & Warszynski, P. (1990) *J. Colloid Interface Sci.* **140**, 123–137.
6. Senger, B., Voegel, J.-C., Schaaf, P., Johnner, A., Schmitt, A. & Talbot, J. (1991) *Phys. Rev. A* **44**, 6926–6928.
7. Senger, B., Schaaf, P., Voegel, J.-C., Johnner, A., Schmitt, A. & Talbot, J. (1992) *J. Chem. Phys.*, in press.
8. Tarjus, G. & Viot, P. (1992) *Phys. Rev. Lett.* **68**, 2354–2357.
9. Huang, Y.-B. & Somasundaran, P. (1988) *Phys. Rev. A* **38**, 6373–6376.
10. Selinger, R. B. & Stanley, H. E. (1990) *Phys. Rev. A* **42**, 4845–4852.
11. Hinrichsen, E. L., Feder, J. & Jøssang, T. (1986) *J. Stat. Phys.* **44**, 793–827.
12. Jullien, R. & Meakin, P. (1992) *J. Phys. A* **25**, L189–L194.
13. Feller, W. (1968) *An Introduction to Probability Theory and Its Applications* (Wiley, New York), Vol. 1, pp. 348–349.